Paper accepted for presentation at 2009 IEEE Bucharest Power Tech Conference, June 28th - July 2nd, Bucharest, Romania

Dynamic Modelling of a grid-connected PEM Fuel Cell in a Distributed Generation Network

P. N. Papadopoulos *Student Member, IEEE*, A. G. Marinopoulos, *Student Member, IEEE*,
G. K. Papagiannis *Member, IEEE*

***Abstract*-- This paper presents a dynamic Proton Exchange Membrane Fuel Cell Model (PEMFC) model based on mass balance and semi-empirical equations. A complete PEMFC System containing a Power Conditioning Unit (PCU) is also investigated and various scenarios are simulated to assess the behaviour of a grid-connected FC in a Distributed Generation (DG) network.**

***Index Terms*-- Fuel cells, distributed energy resources, modelling, power distribution**

I. Introduction

FUEL cells (FC) are electrochemical devices which convert the chemical energy contained in a fuel directly into electricity and heat. They are considered to be suitable for both small and large scale Distributed Generation (DG) applications ranging from a few kW to a few MW.

The most common types of FC used in DG are Solid Oxide Fuel Cells (SOFC), Molten Carbonate Fuel Cells (MCFC) and Proton Exchange Membrane or Polymer Electrolyte Fuel Cells (PEMFC). The main advantages of the FCs are: high efficiency, low or zero emissions when hydrogen is used as a fuel, low noise during operation and high modularity. From the above mentioned types of FCs, the PEMFCs are the most common and widely used. Some of their advantages over other types are: low operating temperature, fast start-up and high current density.

The behaviour of a PEMFC has been reported in many references [1]-[8]. Most of the models are based on the electrochemical description of the phenomena inside the FC. The use of empirical equations is common in order to compute the voltage drop due to various losses [4]. Mass balance equations are used to compute the species changes inside the FC [1], [8]. Finally, energy balance equations are also used especially in high temperature FCs [8], [10].

The interconnection of a FC with the power grid is implemented through Power Conditioning Units (PCU). A PCU consists usually of a dc-dc converter and a dc-ac inverter. Many topologies are proposed in the literature for the PCU [10]. The interaction of FC with the grid is studied in some papers using simple inverter models [1]. More elaborate models for the PCU are given in [5], [11], and [12].

The authors are with the Power Systems Laboratory, Department of Electrical and Computer Engineering, Aristotle University of Thessaloniki, 54124 Thessaloniki, Greece, P.O. Box 486 (phone: +30-2310-996388; e-mail: grigoris@eng.auth.gr).

In this paper a dynamic PEMFC model is proposed in order to investigate the behaviour of a PEMFC connected to a distributed generation network. Various simulations are carried out for different scenarios usually encountered in networks containing distributed generation units, such as partial and full load connection and disconnection and islanded operation. The power performance of the PEMFC is investigated along with the effect of model parameters in the FC operation. The model is implemented in Matlab/Simulink [13], where also the simulations are performed.

II. PEM Fuel Cell Model

The PEMFC under study has an active area of 50 cm^2 and a maximum current density of 1 A/cm^2. The working temperature is considered constant at 70 °C, and the diffusion has not been taken into account as far as its impact on pressure is concerned. Fig. 1 presents the PEMFC model.

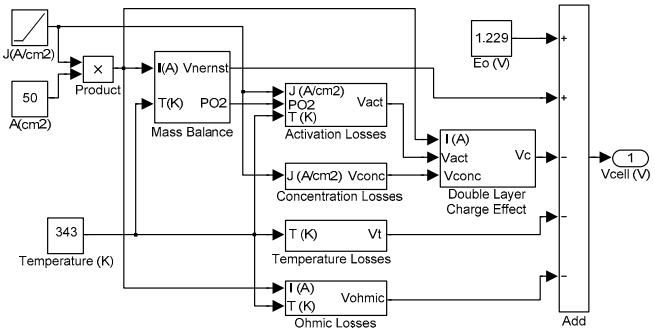

Fig. 1. PEMFC Model built in Simulink.

A. Ideal Cell Potential

The chemical reaction taking place inside a PEMFC when hydrogen is used as a fuel is [9], [10]:

$$H_2 + \frac{1}{2}O_2 \rightarrow H_2O \tag{1}$$

The ideal open circuit potential of the above chemical reaction for standard temperature and pressure (25 °C, 1 atm) and liquid water product is 1.229 V. Using the Nernst equation [9], the open cell potential for different operating pressures and temperatures can be adjusted:

$$E_{nernst} = E^0 + \frac{\Delta S}{2F}(T - T_o) + \frac{RT}{2F}\ln\left(\frac{P_{H_2}\sqrt{P_{O_2}}}{P_{H_2O}}\right) \tag{2}$$

where ΔS is the change in entropy, F is the Faraday constant,

978-1-4244-2235-7/09/$25.00 ©2009 IEEE

R is the universal gas constant, T_o is the standard temperature (278 °K), T is the working temperature in °K and P_{H_2}, P_{O_2} and P_{H_2O} are the partial pressures of the reactant and product species inside the fuel cell [9].

B. Mass Balance Equations

The changes in the partial pressures inside the fuel cell can be determined using the ideal gas law [1], shown in (3). It is assumed that the only gas inside the anode inlet is pure hydrogen, whereas only oxygen is inserted in the cathode inlet. Water is also formed inside the cathode [1], [8].

$$\frac{dp_{H_2}}{dt} = \frac{RT}{V_a}(q_{H_2}^{in} - q_{H_2}^{out} - q_{H_2}^{r}) \tag{3}$$

where p_{H_2} is the partial pressure inside the fuel cell in atm, V_a is the anode volume in L, $q_{H_2}^{in}$ is the hydrogen inlet flow rate in mol/s, $q_{H_2}^{out}$ is the part of the hydrogen that does not react and remains in the cell at this point and $q_{H_2}^{r}$ is the hydrogen that reacts:

$$q_{H_2}^{r} = \frac{I}{2F} \tag{4}$$

From (4) the amount of hydrogen needed can be computed. Usually there is an excess of hydrogen inside the fuel cell.

The partial pressure of the hydrogen is linearly depended on the hydrogen flow:

$$\frac{q_{H_2}}{p_{H_2}} = \frac{K_a}{\sqrt{M_{H_2}}} = K_{H_2} \tag{5}$$

where K_{H_2} is the hydrogen molar flow constant given in mol/(s·atm) [2], [9]. Using the Laplace transformation:

$$p_{H_2} = \frac{1/K_{H_2}}{1+\tau_{H_2}s}(q_{H_2}^{in} - q_{H_2}^{out}) \tag{6}$$

where:

$$\tau_{H_2} = \frac{V_a}{K_{H_2}RT} \tag{7}$$

Eq. (3)-(7) can be used on the cathode side for the determination of the partial pressure of oxygen and water taking into account that the inlet flows are different. The oxygen inlet is half the hydrogen inlet and zero water input both in the anode and cathode side is assumed. In reality the inlet flows contain more gases such as CO, CO2 and probably other hydrocarbons in the anode and nitrogen and other substances contained in the air in the cathode. Both inlet gas streams are often humidified before entering the fuel cell.

As mentioned before, there is an excess of hydrogen in the anode and an excess of oxygen in the cathode. The fuel utilization is a measure that gives the percentage of the fuel consumed inside the fuel cell. The rest of the fuel can be recirculated under certain circumstances. A small amount is lost due to back diffusion through the electrolyte. The utilization is preferably kept around 0.8 to prevent fuel overusage leading to fuel starvation or fuel underusage leading to an increase in voltage output [7].

C. Operating Voltage

When current is drawn from the FC the voltage drops due to various losses. Even when there is no current output, the real open circuit voltage is less than the ideal because of certain losses occurring at zero current. The different types of losses are given below:

1) *Activation Losses* are due to the slow rate of the reaction. The Tafel equation is usually used in order to compute the activation voltage drop [9]. Semi-empirical equations are also commonly used for the computation. In the present work the following semi-empirical equation has been used [3]:

$$\eta_{act} = -0.9514 + 0.00312T - 0.000187T\ln(i) + 7.4\cdot10^{-5}T\ln(c_{O_2}) \tag{8}$$

where T is the temperature in ºK, i is the current density in A/cm^2 and c_{O_2} is the oxygen concentration. The oxygen concentration is calculated by the following semi-empirical equation, after taking into consideration the pressure in the flow channels, diffusion in the electrodes and diffusion through a water film that is created by the presence of water in the electrodes [3]:

$$c_{O_2} = \frac{p_{O_2}}{5.08*10^6\exp(\frac{-498}{T})} \tag{9}$$

2) *Ohmic Losses* come mainly from the ionic resistance of the electrolyte and from the electronic resistance of the electrodes, interconnections and other parts of the FC [9]. The membrane specific resistance in Ω·cm is computed using the following empirical equation [4]:

$$r_m = \frac{181.6[1+0.03\frac{i}{A}+0.062(\frac{T}{303})^2(\frac{i}{A})^{2.5}]}{(\lambda-0.634-3\frac{i}{A})\exp(4.18\frac{T-303}{T})} \tag{10}$$

where i is the current in A, A is the active cell area in cm^2, T is the temperature in °K and λ is an empirical parameter that shows the humidity percentage in the membrane. Parameter λ ranges from 14, when the membrane is considered 100% humidified, to 23, when the membrane is considered "flooded". To compute the resistance of the membrane in Ω the following expression is used:

$$R_m = \frac{r_m * l}{A} \tag{11}$$

where l is the width of the membrane in cm. Nafion 117 is used as a membrane material with a width of 178 μm [6].

3) *Concentration Losses* are caused by the depletion of the reactants in the reaction sites and occur in high current densities. The voltage drop due to these losses is computed using the following semi-empirical equation [6]:

$$\eta_{conc} = -B\ln(1-\frac{i}{i_{\max}}) \tag{12}$$

where i is the current density in A/cm^2 and i_{max} is the maximum current density of the fuel cell. The maximum

current density that the fuel cell can withstand is assumed to be 1 A/cm^2.

4) *Charge Double Layer Effect.* In the contact surface of the electrode and the electrolyte some charge is built up due to diffusion effects and due to reactions between the electrons in the electrodes and the protons in the electrolyte. This acts like a capacitor which smoothes the voltage drop due to the activation and the concentration losses [6], [8]. The capacitance is usually in the order of a few Farads [6] and in the present model is considered to be 1.5 F.

The modelling parameters that were used to construct the PEMFC model are shown in Table I.

TABLE I
MODELLING PARAMETERS

Modelling Parameter	**Value**
Effective Cell Area A	50 cm^2
Membrane Width	178 μm
Temperature T	343 °K
Ideal Voltage E_o	1.229 V
Hydrogen molar constant K_{H_2}	$4.7955 \cdot 10^{-7}$ kmol/(atm·s)
Oxygen molar constant K_{O_2}	$2.39773 \cdot 10^{-7}$ kmol/(atm·s)
Water molar constant K_{H_2O}	$8.768 \cdot 10^{-8}$ kmol/(atm·s)
Maximum current density J_{max}	1 A/cm^2
Constant λ	14<λ<23
Constant B	0.016 V
Anode Volume	0.0454 L
Cathode Volume	0.0454 L

D. V-I and P-I Curves

Using the model described above, the V-I curve shown in Fig. 2 is derived. For low currents the main losses are the activation losses. There is also a linear drop in voltage, mainly due to the ohmic losses, and at high operating currents a sharp voltage drop due to the concentration losses. In Fig. 3 the derived P-I curve is shown. The maximum power output of the fuel cell does not appear at maximum current, but at around 80% of maximum load and is approximately 24 W.

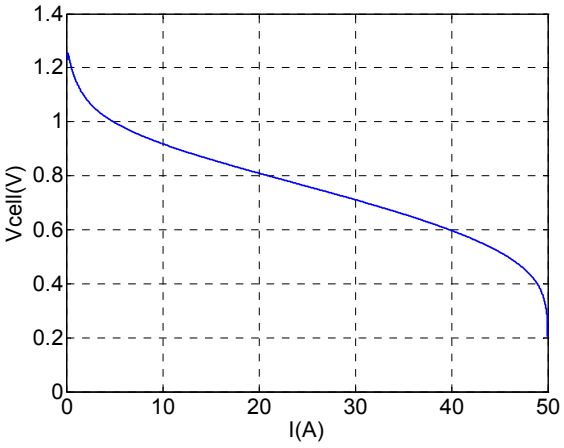

Fig. 2. V-I curve.

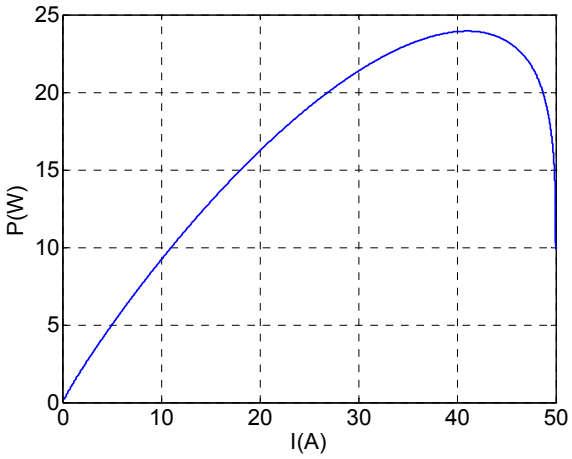

Fig. 3. P-I curve.

III. TEST NETWORK

A. Simulink Model

A fuel cell stack consisting of 300 fuel cells connected in series is used to model the interaction with the DG network. The maximum power output is around 7200 W. No extra losses are considered for the stack. A model of a PCU connecting the fuel cell stack to the grid has been build using Simulink, as shown in Fig. 4.

A simple dc-dc boost converter was used to boost the output voltage of the fuel cell stack at 300 V. A PI controller monitors the mean dc voltage output and sends PWM signals to the switch of the boost converter. The switch is considered to be a MOSFET with operating resistance 0.01 Ohms.

A 3-phase dc-ac inverter using Sinusoidal Pulse Width Modulation (SPWM) converts the dc voltage into 3-phase, 50 Hz, 130 V rms phase to phase. The switches of the inverter are MOSFETs with 0.01 Ohm resistance. A snubber resistance and capacitance are also considered to ensure numerical stability. Furthermore, a LC filter is connected to the output terminals of the inverter in order to reduce harmonics. Since the switching frequency is considered to be 2550 Hz an inductance of 2 mH and a capacitance of 753 uF, which give a cut-off frequency of 130 Hz, are more than enough.

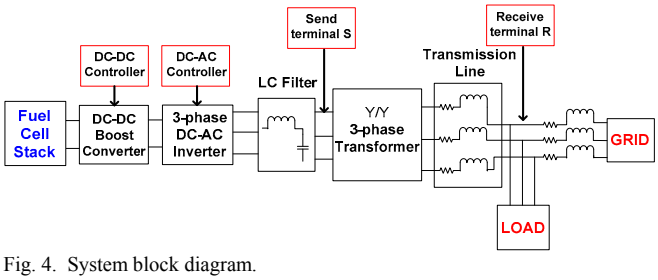

Fig. 4. System block diagram.

The control scheme of the inverter, illustrated in Fig. 5, is described below: first the amplitude and phase of the 3-phase load voltage is measured and a dq transformation is applied. The desired active and reactive power output of the FC system

as well as the desired voltage amplitude are inserted and using (13) and (14) an ideal 3-phase voltage is created. $Z<y^o$ is the impedance between the send terminal S and the receive terminal R, which are shown in Fig. 4, and δ is the angle between V_S and V_R. The dq transformation is also applied and the difference between the desired dq signal and the measured one are inserted into a PI controller which gives the appropriate signals to a PWM generator block.

$$P_R = \frac{V_R V_S}{Z}\cos(y-\delta) - \frac{V_R^2}{Z}\cos(y) \quad (13)$$

$$Q_R = \frac{V_R V_S}{Z}\sin(y-\delta) - \frac{V_R^2}{Z}\sin(y) \quad (14)$$

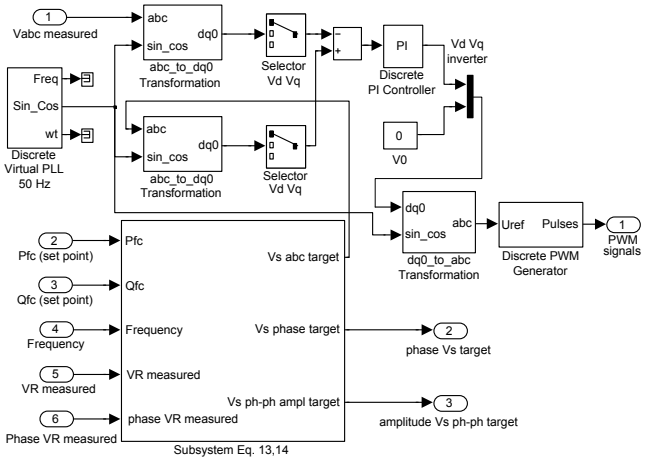

Fig. 5. Control scheme.

A Y-Y transformer is used to step up the voltage at 400 V phase to phase. Typical parameters are used to model the transformer. Finally, a 5 km RL transmission line connects the system to the low voltage side of a power distribution network. The overall resistance is considered to be 2.568 Ohms and the inductance 5 mH. The distribution network is modelled using a 400 V voltage source connected in series with a resistance of 0.1 Ohms and an inductance of 3 mH. The model is implemented using the Power System Blockset of Simulink.

B. Simulation

Various simulations have been carried out using the above model in order to observe the dynamic behaviour of the FC system during transients. The FC model presented in Section II is suitable for transient studies but within the operating region of the FC because there are problems with the voltage output when the current exceeds the maximum operating current limit of 50 A. The response of the FC alone is several seconds but the whole system is much faster. The changes shown below happen before the FC reaches its steady state.

1) Scenario A Isolated Load

- Starting from t=0 s, the FC model takes one second to start-up.
- At t=1 s the FC is connected to an isolated load, providing 1 kW of real power to a load demanding also 1 kW.
- At t=3 s a 4.5 kW, 3 kVAr load is connected and the FC system output power is set to provide 5.5 kW real power and 3 kVAr reactive power.
- At t=5 s the above load is disconnected. The FC is set to provide 1 kW.

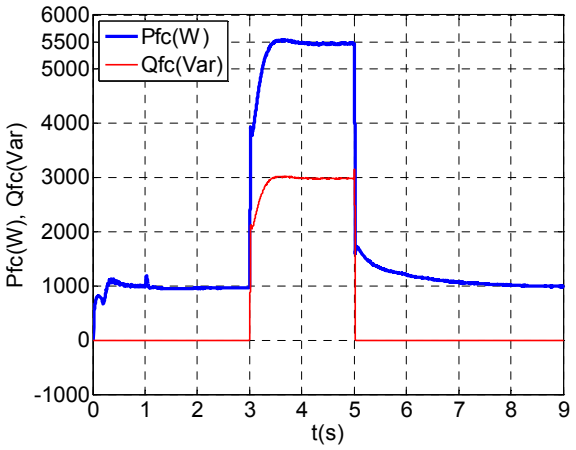

Fig. 6. Fuel cell system active and reactive power output for Scenario A.

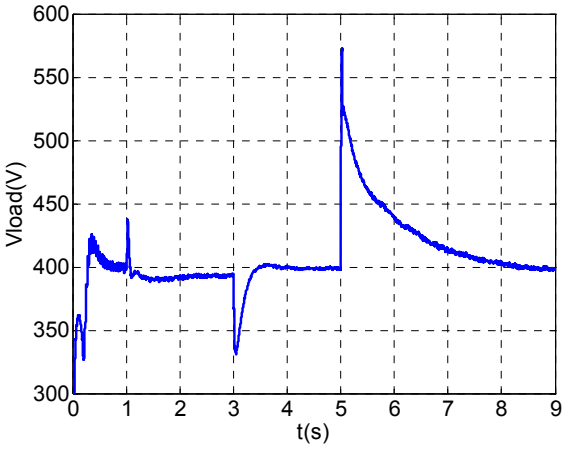

Fig. 7. Load Voltage for Scenario A.

As we can see in Fig. 6 when the load is connected the FC output power changes smoothly and reaches steady state in around 0.5s without elevation both for the active and the reactive power. The reactive power though settles a little faster. The voltage, which is shown in Fig. 7 dips at around 330 V which is more than 17% but for less than 0.5 s.

On the contrary when the load is disconnected the transient lasts for around 3s and the voltage spike reaches a very large value of around 570 V which can cause serious damage to the power electronics of the boost converter and inverter. This spike is also present at the dc bus voltage and it has to do mainly with the converter controllers but also with the sudden pressure rise inside the FC anode.

2) Scenario B Grid connected operation

- Starting from t=0 s, the FC model takes one second to start-up.
- At t=1 s the FC is connected to the grid, providing 1 kW of real power to a load demanding also 1 kW.
- At t=3 s a 4.5 kW, 3 kVAr load is connected and the FC system output power is set to provide 5.5 kW real power and 3 kVAr reactive power.
- At t=5 s the above load is disconnected. The FC is set to provide 1 kW.

This scenario is the same with Scenario A with the difference that the FC is also connected to the grid. Here the transient is a little more intense as shown in Fig. 8. The real power output needs approximately 1 s to reach steady state and a small elevation of around 400 W, about 7%, is also present. The same applies for the reactive power but it reaches steady state a little faster than before with a larger elevation of around 450 Var, which is about 15%. The load disconnection shows no problem. The voltage, which is shown in Fig. 9, is supported by the grid and there is only a very small drop or rise during transients. No dips or over- voltages are recorded.

In Fig. 10 we can see that, when there is a load connection and disconnection at the same time in which the FC set-point changes, there is a large spike in both the active and reactive power of the grid. This happens because the response of the grid to load changes is faster than the FC system and tries to provide or absorb the power needed until the FC system regulates its output. The grid reactive power changes a little faster than the active power. It should be noted that both the active and the reactive grid power are considered positive when they flow from the local loads.

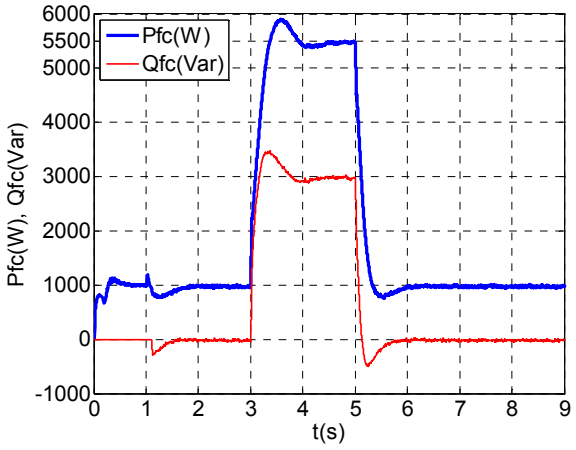

Fig. 8. Fuel cell system active and reactive power output for Scenario B.

3) Scenario C Step changes and compensation

- Starting from t=0 s, the FC model takes one second to start-up.
- At t=1 s the FC is connected to the grid, providing 1 kW of active power to a load demanding also 1 kW.
- At t=3 s the FC output power is increased to 3 kW while the load remains 1 kW. The excess power is provided to the grid.
- At t=5 s a 3.5 kW, 2 kVAr load is connected. The FC power output is increased to 5.5 kW and the extra 1 kW active power is provided to the grid. The grid provides 2 kVAr reactive power to the load.

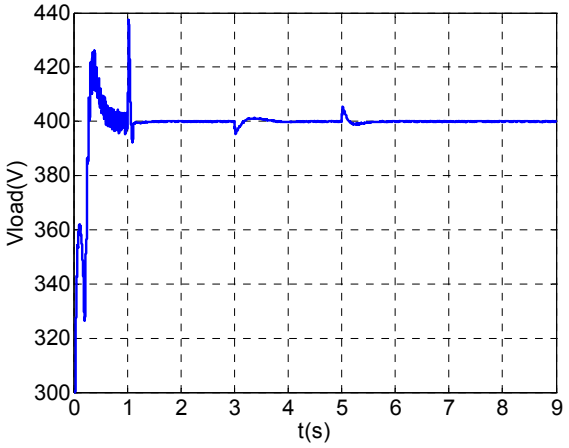

Fig. 9. Load Voltage for Scenario B.

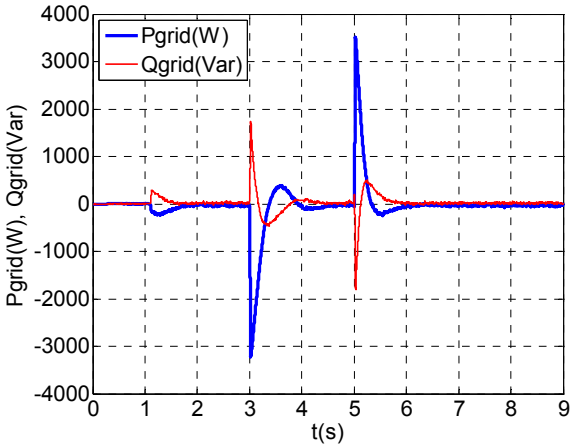

Fig. 10. Active and reactive grid power for Scenario B.

- At t=7 s a 5 kW, 4 kVAr load is connected while the FC continues to provide 5.5 kW. The excess real and reactive power needed is provided by the grid.
- At t=9 s the FC system is set to compensate for 5kVAr reactive power while continuing to provide 5.5 kW active power. The excess active and reactive power needed is again provided by the grid.

Fig. 11 shows the active and reactive power output of the fuel cell system. The system needs approximately 0.5 s for small load changes and 1 s for heavy load changes to reach steady state condition both for active and reactive power. We can also see a drop in the real power of around 1 kW at t=9 s when the fuel cell is set to compensate some reactive power.

This has to do mainly with the sudden increase in the current and the slow response of the voltage controller.

Fig. 12 shows the active and reactive power of the grid. During transients it takes 0.5 s for the grid active and reactive power to reach steady state. The response of the gird is generally faster than that of the FC system.

This can be clearly seen at t=5 s when a load is connected with a simultaneous change in the FC set point as mentioned in Scenario B. A similar spike is not noticed when there is a change in the FC set point but the load remains constant at t=3 s. At t=9 s there is also an increase in the grid active power of around 1 kW because of the respective drop in the FC system output.

The load voltage, shown in Fig. 13, drops when the grid is heavily loaded either providing or absorbing power. The voltage drops at 385 V at t=7 s and is increased at 396 V at t=9 s when the FC compensates some reactive power. We can also see that when the voltage drops the grid provides less power to the loads than needed. When the FC compensates the reactive power, the real power provided by the grid changes from 3.4 kW to 3.9 kW, closer to what is required by the load, because of the voltage correction.

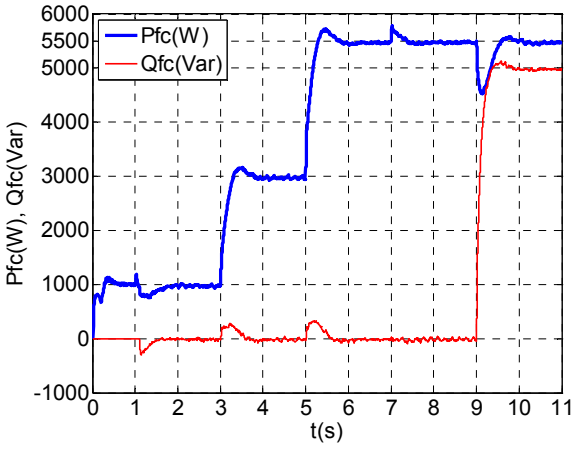

Fig. 11. Fuel cell system active and reactive power output for Scenario C.

4) Scenario D: Light loaded islanding operation

- Starting from t=0 s, the FC model takes one second to start-up.
- At t=1 s the FC is connected to the grid, providing 1 kW of real power to a load demanding also 1 kW.
- At t=3 s a 4.5 kW, 3 kVAr load is connected and the FC system output power follows the load.
- At t=5 s the grid is disconnected. The FC is working in islanded mode for 500 ms and then the gird is connected again.

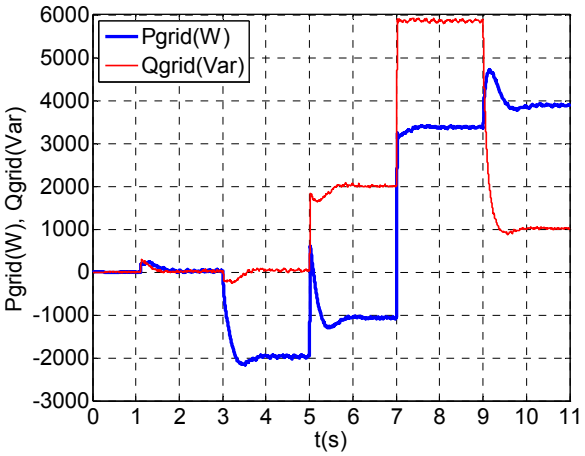

Fig. 12. Active and reactive grid power for Scenario C.

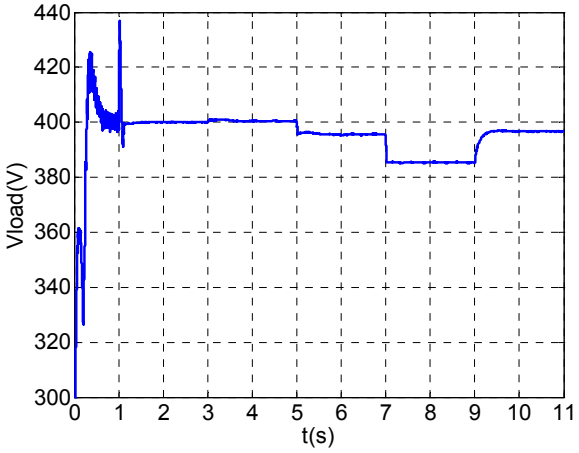

Fig. 13. Load Voltage for Scenario C.

In this scenario the FC provides active and reactive power to local loads within the operating range of the FC system as shown in Fig.14 and 15. At t=3 s we can see the spikes in Fig. 15 mentioned in scenarios B and C. At t=5 s when the grid is disconnected the FC can withstand the local loads and it continues to provide active and reactive power uninterruptedly. The load voltage, presented in Fig. 16, shows some ripple because it is no longer supported by the grid. After 500ms the grid is connected again without any problems. No stability issues are recorded for the FC. However care must be taken at grid connection because the inverter can be desynchronized.

5) Scenario E Heavy loaded islanded operation

- Starting from t=0 s, the FC model takes one second to start-up.
- At t=1 s the FC is connected to the grid, providing 1 kW of real power to a load demanding also 1 kW.
- At t=3 s a 8 kW, 5 kVAr load is connected and the FC system output power is set to provide 5.5 kW real power and 3 kVAr reactive power.

- At t=5 s the grid is disconnected. The FC is working in islanded mode for 500 ms and then the grid is connected again.

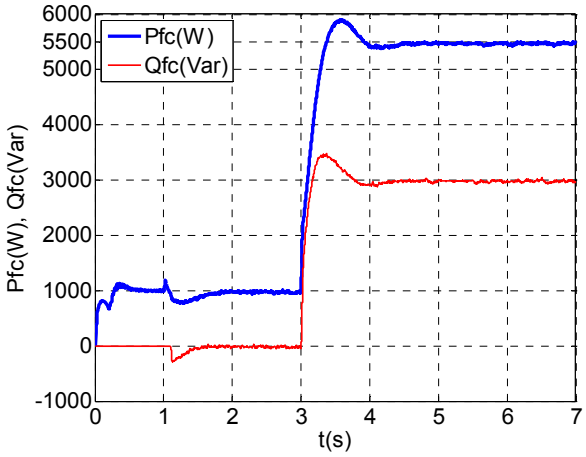

Fig. 14. Fuel cell system active and reactive power output for Scenario D.

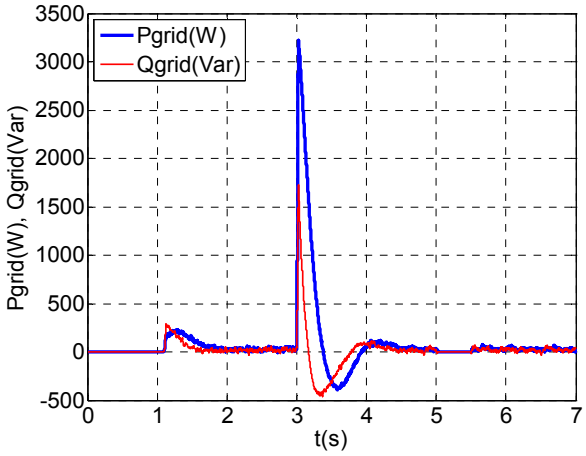

Fig. 15. Active and reactive grid power for Scenario D.

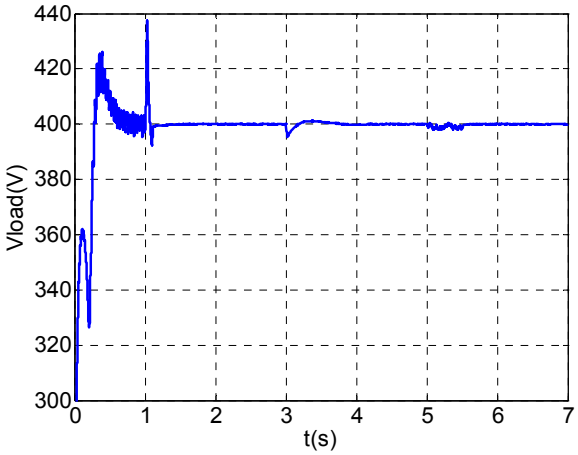

Fig. 16. Load Voltage for Scenario D.

Fig. 17 shows the active and reactive power of the FC system and Fig. 18 shows the active and reactive power of the grid. At t=3 s we can notice the large spike in the grid active and reactive power mentioned in scenarios B and C. At t=5 s the grid is disconnected and the FC is operating in island mode but the load demand is higher than the FC set point. At first there is a slight increase in both active and reactive power but the system cannot provide all the power needed and the output starts to decline. The voltage, which is shown in Fig. 19, drops at around 320 V when operating in island mode, which is unacceptable.

After 500 ms the grid is connected again and the voltage returns to its initial value. After a short transient period of around 0.5 s the active and reactive power of both the FC and the grid reaches steady state. Similar spikes to that mentioned in the scenarios B and C can also be noticed for the reactive power. No stability problems occur for the short period of time that the FC is operating in island mode. However for longer disconnection times the angle of the controlled inverter voltage increases linearly and leads to a very large reverse power from the grid to the FC system which may cause damage to the power electronics.

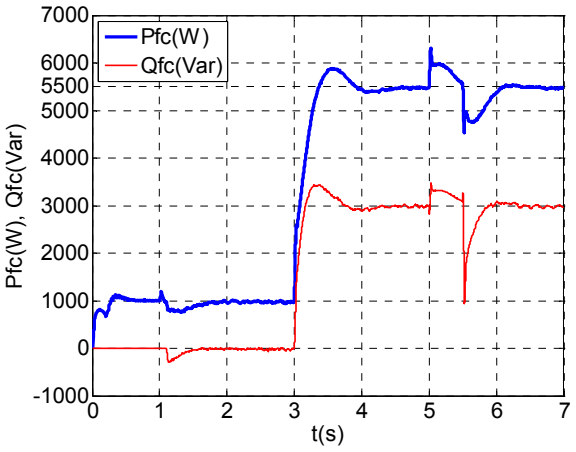

Fig. 17. Fuel cell system active and reactive power output for Scenario E.

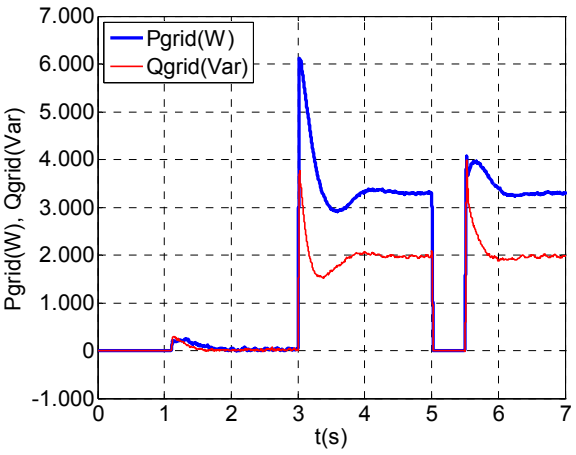

Fig. 18. Active and reactive grid power for Scenario E.

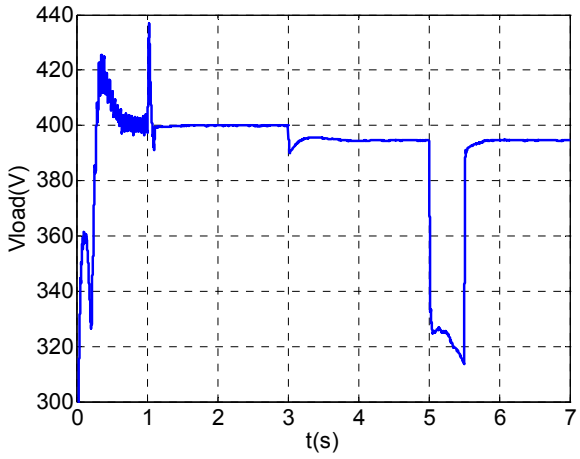

Fig. 19. Load Voltage for Scenario E.

IV. Conclusion

A FC model is presented along with a PCU to connect the FC to the grid. The FC model is based on semi empirical and mass balance equations and the PCU consists of a dc-dc boost converter, a dc-ac inverter and an output LC filter. Finally a transformer and an RL line are used to connect the FC system to the low voltage grid. Isolated load operation, grid connected operation and islanding scenarios are simulated to investigate the behaviour of the system during transients conditions commonly encountered in DG networks.

During islanded operation the output voltage shows a small ripple and problems have been recorded at load disconnection. The use of a backup power source can stabilize the system, especially when there is a reformer involved. When the FC is connected to the grid the voltage is supported and there is no need for a backup power source during transients, since the grid controls the surplus power.

In islanded operation the FC can provide power to local loads but only within its operating range and for small time intervals of around 500 ms. Care should be taken to ensure that the inverter is synchronized with the grid when it is connected again. For longer time spans the problem is more severe and large amounts of power can flow into the FC system damaging the equipment. Islanding should be generally avoided because, if overloaded, the FC could suffer from fuel starvation and the voltage drop is unacceptable.

Some general remarks are that when the FC system operates within its limits it can provide active and reactive power to local loads and to the grid to cover power demand at other sites or to compensate some reactive power supporting the load voltage. The voltage drop remains within acceptable range except for some cases of heavy loading. There are no stability issues concerning the FC but there are some restrictions in the operating current due to the use of empirical equations. A more suitable FC model should be developed to simulate transients with very high currents.

V. References

[1] M. Y. El- Sharkh, A. Rahman, M. S. Alam, P. C. Byrne, A. A. Sakla, T. Thomas, "A dynamic model for a stand-alone PEM fuel cell power plant for residential applications", *Journal of Power Sources*, Vol. 138, 2004, pp. 199-104.

[2] M. Uzunoglu, M. S. Alam, "Dynamic Modeling, Design, and Simulation of a combined PEM Fuel Cell and Ultracapacitor System for Stand-Alone Residential Applications", *IEEE Transactions on Energy Conversion*, Vol. 21, No. 3, 2006, pp. 767 – 775.

[3] J. C. Amphlett, R. M. Baumert, R.F Mann, B. A. Peppley, P. R. Roberge, T.J. Harris, "Performance Modeling of the Balard Mark IV Solid Polymer Electrolyte Fuel Cell Part I. Mechanistic Model", *Journal of Electrochemical Society*, Vol. 142, No. 1, 1995, pp. 1 – 8.

[4] R. F. Mann, J. C. Amphlett, M. A. I. Hooper, H. M. Jensen, B. A. Peppley, P. R. Roberge, "Development and application of a generalised steady-state electrochemical model for a PEM fuel cell", *Journal of Power Sources*, Vol. 86, 2000, pp. 173 – 180.

[5] M. J. Khan, M. T. Iqbal, "Dynamic Modeling and Simulation of a Fuel Cell Generator", *Wiley Fuel Cells*, 5, No.1, 2005, pp. 97 – 104.

[6] J. M. Correa, F. A. Farret, L. N. Canha, M. G. Simoes, "An Electrochemical-Based Fuel-Cell Model Suitable for Electrical Engineering Automation Approach", *IEEE Transactions on Industrial Electronics* Vol. 51, No. 5, 2004, pp. 1103 - 1112.

[7] K. Sedghisigarchi, A. Feliachi, "Control of Grid-Connected Fuel Cell Power Plant for transient stability enhancement", *IEEE Power Engineering Society Winter Meeting*, Vol. 1, 2002, pp 383-388.

[8] C. Wang, M. H. Nehrir, S. R. Shaw, "Dynamic Models and Model Validation for PEM Fuel Cells Using Electrical Circuits", *IEEE Transactions on Energy Conversion* Vol.20, No. 2, 2005, pp.442-451.

[9] J. Larminie, A. Dicks, "Fuel Cell Systems Explained", second edition, *John Wiley & Sons* Ltd., 2003.

[10] EG&G Technical Services, "Fuel Cell Handbook (Seventh Edition)", *U.S. Department of Energy*, 2004.

[11] Jin Woo Jung, "Modeling and control of fuel cell based distributed generation systems", Dissertation, *Ohio State University*, 2005.

[12] Jin-Woo Jung, Al Keyhani, "Control of a Fuel Cell Based Z-Source Converter", *IEEE Transactions on Energy Conversion*, vol.21, No. 2, June 2007.

[13] MATLAB™, Version 2007b, http://www.mathworks.com.

VI. Biographies

Panagiotis N. Papadopoulos (S'05) was born in Komotini, Greece, on March 30, 1985. He received the Dipl. Eng. Degree from the Department of Electrical and Computer Engineering at the Aristotle University of Thessaloniki, in 2007.

Since 2007 he has been postgraduate student at the same university. His research interests are in the field of power system modelling, simulation and transient analysis and distributed generation.

Antonios G. Marinopoulos (S'04) was born in Thessaloniki, Greece, on July 10, 1980. He received the Dipl. Eng. Degree from the Department of Electrical and Computer Engineering at the Aristotle University of Thessaloniki, in 2003.

Since 2004 he has been postgraduate student with the same university. His research interests are in the field of power system analysis and their simulation, distributed generation and electromagnetic transients.

Grigoris K. Papagiannis (S'79-M'88) was born in Thessaloniki, Greece, on September 23, 1956. He received his Dipl. Eng. Degree and the Ph.D. degree from the Department of Electrical and Computer Engineering at the Aristotle University of Thessaloniki, in 1979 and 1998 respectively.

He is currently As. Professor at the Power Systems Laboratory of the Department of Electrical and Computer Engineering of the Aristotle University of Thessaloniki, Greece. His special interests are power systems modelling, computation of electromagnetic transients, distributed generation and powerline communications.